Segregation of Admixing Elements in The Boundary Layer of the Main Inlet of a Ductile Iron Casting

B. Borowiecki *, S. Mak

Faculty of Mechanical Engineering and Mechatronics, West Pomeranian University of Technology in Szczecin,
al. Piastów 19, 70-310 Szczecin, Poland
*Corresponding author. E-mail address: Boguslaw.Borowiecki@ps.pl

Abstract

The object of the present paper is to determine the distribution of admixing elements, such as magnesium, manganese, silicon and sulfur, in the boundary layer of the main inlet of a ductile iron casting. The authors also intend to demonstrate the influence of elements diffusing from the casting mold, such as oxygen and silica, on the chemical composition of the boundary layer of the casting.

1. Introduction

Considering the superior strength characteristics, ductile iron is a known and valued construction material. It is in common usage since the fifties of the past century. It's excellent mechanical properties, such as a high tensile strength, compression and bending strength, as well as a good susceptibility to plastic working, opened the possibility of reducing the wall thickness of the castings, which can be directly connected with the weight reduction of the produced elements.

The phenomenon of segregation has an adverse effect on the mechanical properties of this alloy and is based on a non-uniform distribution of elements in the casting volume during non-equilibrium solidification – it results from the difference in the chemical composition of the solid and the liquid phases (in the various stages of the solidification process, the phases crystallize at a different speed) [1], [2]. This phenomenon is undesirable and results in a downgrade of the casting's mechanical properties, especially if we take the small wall thickness into account. The

degree of segregation depends on the temperature and pouring speed of the cast iron, on the casting's wall thickness, the degree of supercooling, and hence, the linear crystallization velocity and the number of the crystallization nuclei [1, 4, 6].

In this paper we will show the quantitative character of the segregation phenomenon of admixing elements in the boundary layer of a ductile iron sample, taken from the casting's main inlet. In addition, we will show the influence of the reaction of compounds contained in the mold on the chemical composition of the sample's boundary layer, since the elements contained in the mold can have undesirable effects on the casting, causing the formation of gas pockets inside the component [5, 7].

For imaging purposes of the element segregation in the casting, a scanning electron microscope (SEM) was used. The techniques of backscattered electrons (BSE), secondary electrons (SE) and energy-dispersive X-ray spectroscopy (EDS) were employed. The BSE and SE techniques were used to show the microstructure of the sample's cross section. Images obtained by the EDS show the scattered distribution of atoms (molecules) of the given element on the sample's cross-section surface, the

quantitative distribution of elements at a given point and the distribution profile of elements along a line.

2. Examined sorts of cast iron

A fragment of the main inlet of a ductile iron casting of the sort EN-GJS 507 was examined. The sample was taken from the lower part of the main inlet with a circular cross section of ∅22. The temperature of the liquid cast iron amounts to 1318 ^oC. The pouring time was 5s. The moisture content in the casting mold amounts to 3,44%, the compression strength was 2,34 N/cm^2. Table 1 shows the chemical composition of the examined cast iron sample:

Table 1.
Content of admixing elements in the sample for SEM analysis

C	Si	Mn	Mg
3,75%	2,72%	0,22%	0,057%
S	F	Al	
0,021%	0,051%	0,012%	

As it is shown in the table, the object of research is unalloyed ductile iron, which uses magnesium as a spheroidizing agent. With the help of the BSE technique, a microstructure image of the examined sample was obtained:
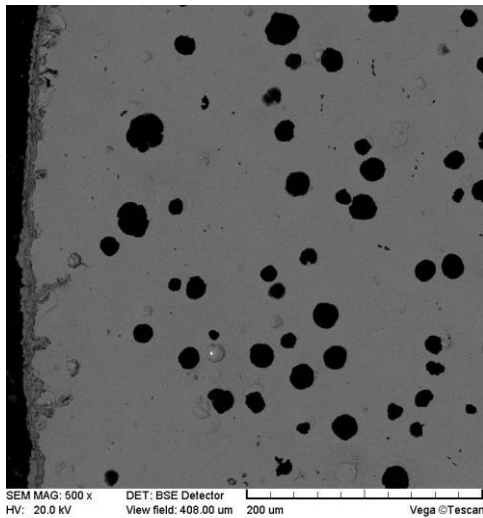

Fig. 1. Distribution of graphite nodules on the sample's cross section, magnification 200x
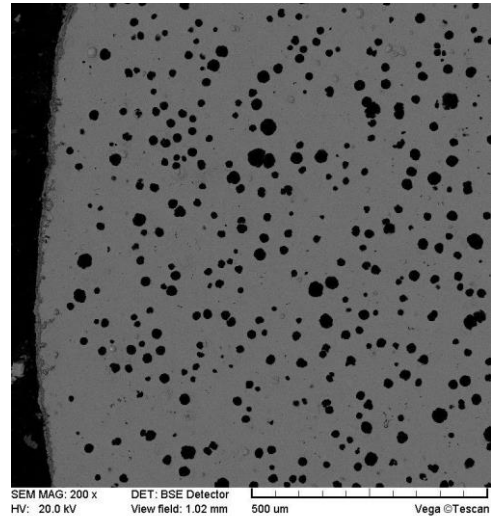

Fig. 2. Distribution of graphite nodules on the sample's cross section, magnification 500x

As can be seen, the amount of graphite precipitations is relatively large, with a relatively small diameter in the order of 20μm. In conclusion, the distance between the graphite nodules must also be small, in the order of 50μm. It can be seen, that the graphite precipitations are present in the immediate vicinity of the casting's wall, approximately at a distance of 60μm.

3. Segregation of admixing elements

3.1. Distribution profile of elements along a line

With the help of the scanning microscope technique, the following distribution of elements along a line with a length of 400μm in the sample was obtained, fig. 3 and fig. 4:
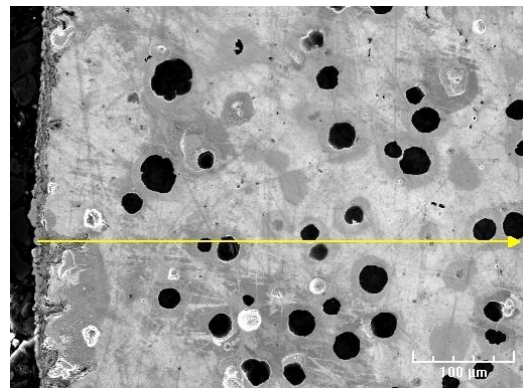

Fig. 3. View of the sample's cross section with plotted line for the spectral analysis
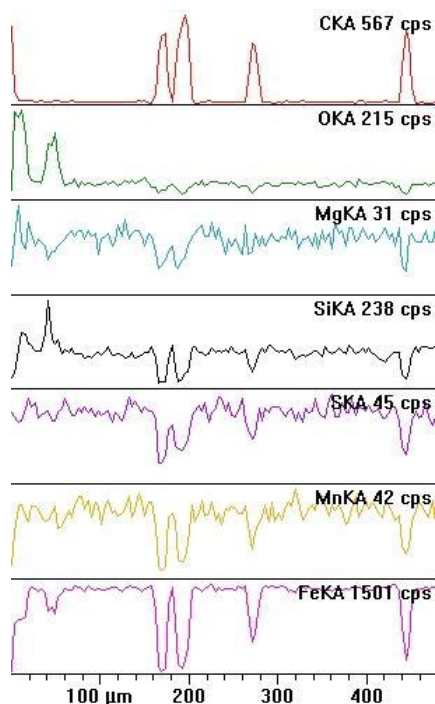
Fig. 4. Linear distribution of elements in the sample

As can be seen, the carbon content decreases from the sample's wall and is more or less constant in the distal section, then increases rapidly in the places where the graphite precipitations are located [7].

The oxygen content is at it's peak at the place of contact with the casting mold. On the contrary, the iron content shows it's minimum at this very place. This can be explained by the influence of moisture contained in the casting mold. Moisture permeates from the mold into the casting and reacts with the iron to form iron oxide. Hence, in the outer layer of the cast iron sample the following reaction occurs:

$$Fe + H_2O \rightarrow FeO + H_2 \qquad (1)$$

The silicon content is at it's smallest at the wall of the sample, then it remains more or less constant over the whole length of the cross-section, decreasing rapidly in places of graphite precipitations. Silicon forms fayalite, which is a result of the reaction of iron oxide with the silica contained in the casting mold:

$$2FeO + SiO_2 \rightarrow 2FeO \cdot SiO_2 \qquad (2)$$

On the other hand, magnesium shows it's largest presence at the contact place with the mold, maintaining further a constant level. Around the precipitations of graphite an increased amount of magnesium can be observed. The minimum magnesium content is present in the graphite nodules.

In the outer layer of the sample, trace amounts of manganese can be observed, which maintains a constant and higher level in the further section thereof – with the exception of places, where graphite precipitations are located.

The iron content is at it's smallest at the wall of the sample, whereupon it increases, keeping a constant level. The hydrogen from reaction (1) permeates further into the casting and reacts with cementite, forming methane gas:

$$2H_2 + Fe_3C \rightarrow 3Fe + CH_4 \qquad (3)$$

The sulfur content of the metal matrix oscillates about a constant level, while in the area of graphite precipitations sharp declines in sulfur content can be observed.

3.2 Scattered distribution

In the current subsection we will demonstrate the scattered distribution of elements on the cross-section's surface of the sample.
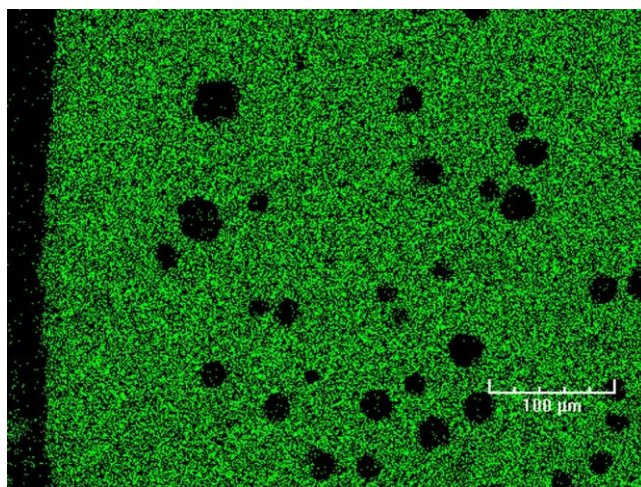

Fig. 5. Segregation of iron in the sample's boundary layer

Iron is distributed uniformly over the sample, a decrease at the boundary of the cross-section is observed.
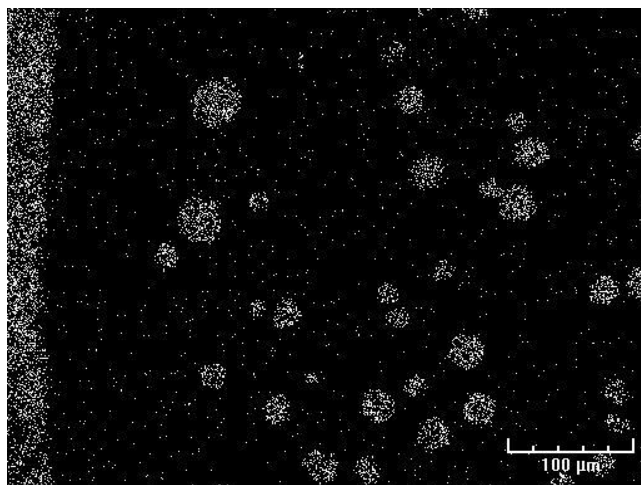

Fig. 6. Segregation of carbon in the sample's boundary layer

As can be seen in figure 6, the boundary layer doesn't show a regular distribution pattern of carbon. However, on the edge of the sample a zone of increased carbon content was observed. This zone has an equal width of approximately 30μm. These are the remains of molding sand adhering to the casting (soot is added to the molding sand). It can be assumed, that the soot reacts with moisture from the molding sand, forming carbon oxide:
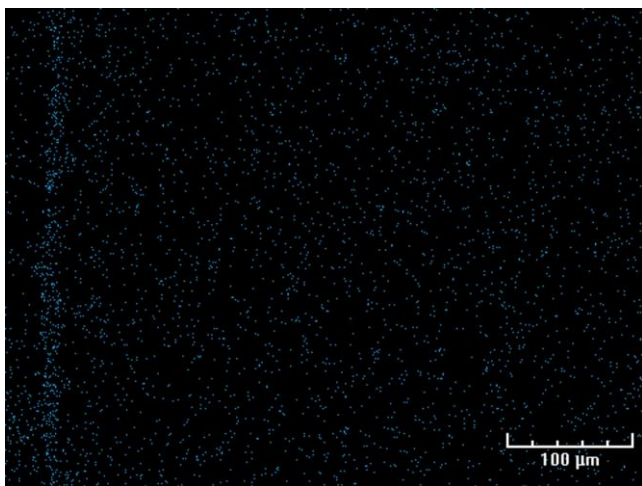
$$H_2O + C \rightarrow CO + H_2 \qquad (4)$$

Fig. 7. Segregation of oxygen in the sample's boundary layer

On the edge of the sample, a zone with increased oxygen content can be found. In the remaining part of the sample, the oxygen content is smaller, showing an uniform distribution pattern. This is explained by the formation of iron oxide and fayalite.
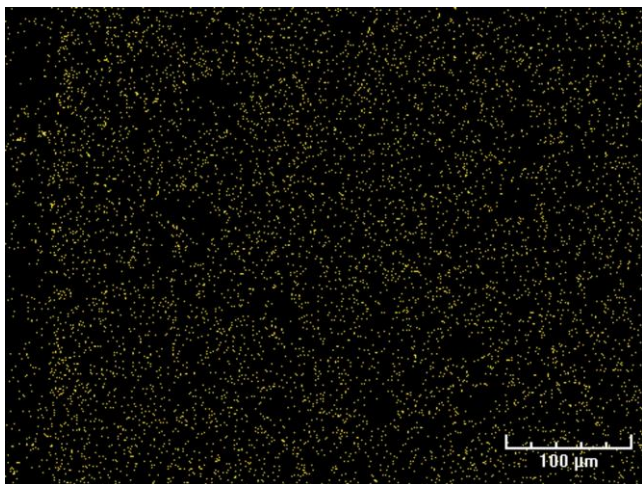

Fig. 8. Segregation of silicon in the sample's boundary layer

The distribution of silicon is uniform throughout the whole cross-section of the sample. A lower concentration of silicon occurs in places occupied by the graphite nodules.
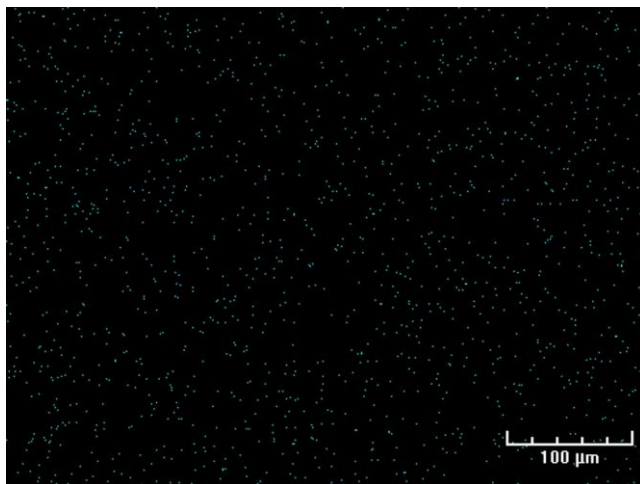

Fig. 9. Segregation of magnesium in the sample's boundary layer

The precipitations of magnesium don't demonstrate an uniform segregation pattern over the sample's entire cross-section. On the other hand, local agglomerations of this element can be seen around the graphite precipitations.
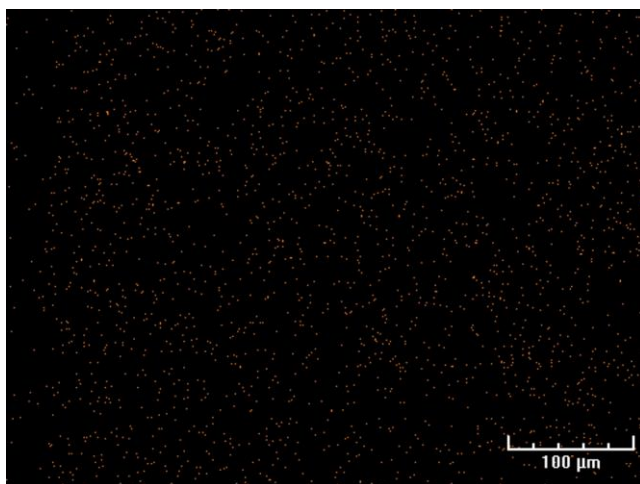

Fig. 10. Segregation of manganese in the sample's boundary layer

The same can be said about the segregation of manganese. Manganese occurs as an element bound to sulfur, according to the reaction:
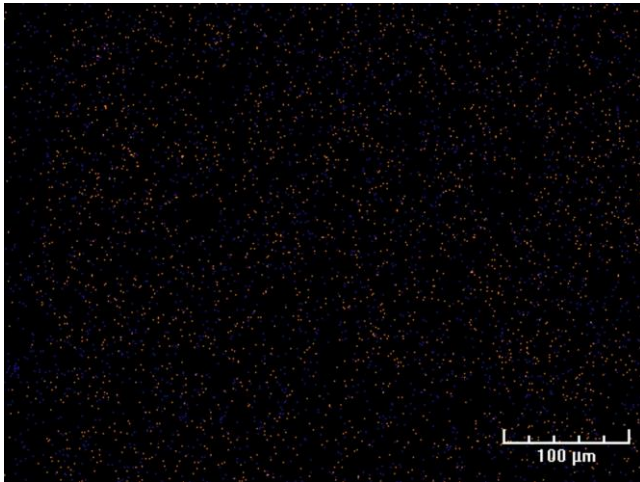
$$FeS + Mn \rightarrow MnS + Fe \qquad (5)$$

Fig. 11. Segregation of sulfur and manganese in the sample's boundary layer

As can be seen on figure 11, manganese occurs in places, where sulfur is present.
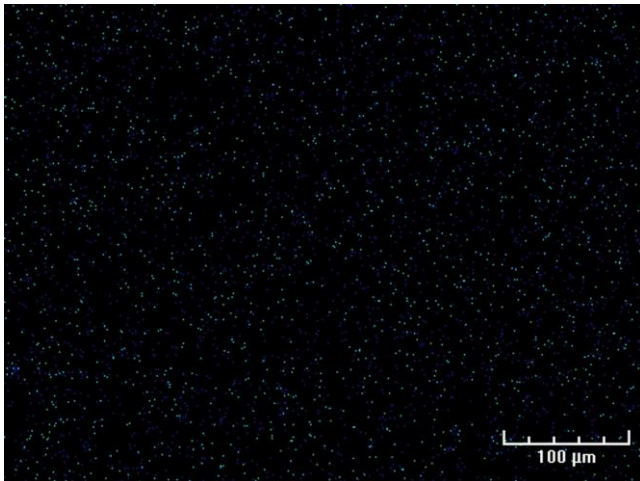

Fig. 12. Segregation of sulfur and magnesium in the sample's boundary layer

Magnesium binds to sulfur, too, as can be seen on figure 12. The binding occurs according to the following reaction:

$$FeS + Mg \rightarrow MgS + Fe \qquad (6)$$

3.3. Point distribution of elements

In the present subsection we intend to demonstrate the sample's chemical composition at several points on it's cross-section. In this way, the change in the chemical composition of the cast iron will be shown, depending on the distance from the sample's border.
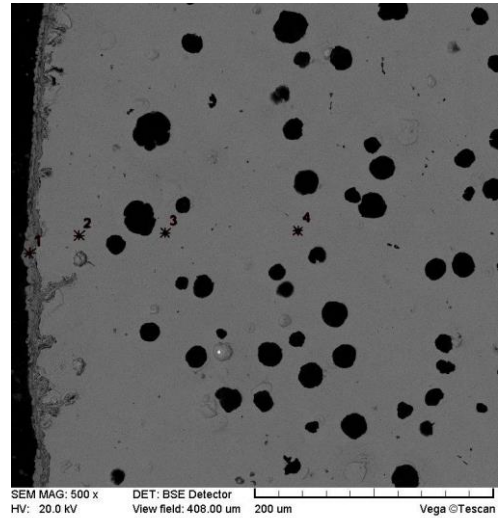

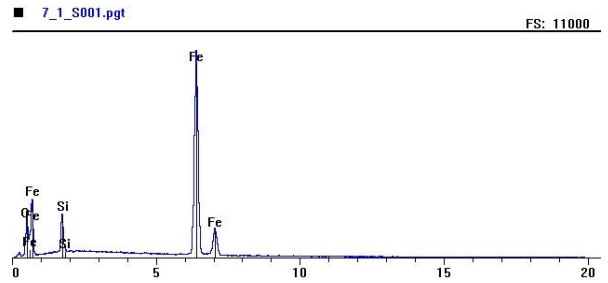Fig. 13. Measuring points on the sample's surface

Fig. 14. Result of EDS-analysis at point 1

Table 2.
Chemical composition of the sample at point 1

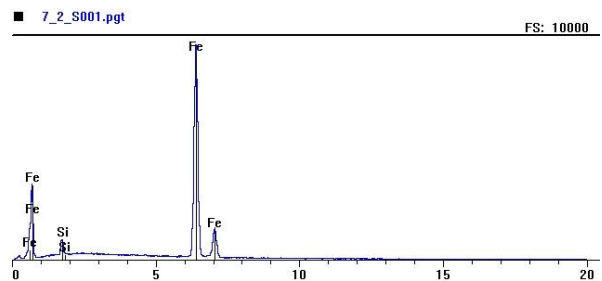| Element	Line	Wt%	At%
O	KA1	13,97	34,64
Si	KA1	6,03	8,53
Fe	KA1	80,00	56,83
Total		**100,00**	**100**

Fig. 15. Result of EDS-analysis at point 2

Table 3.
Chemical composition of the sample at point 2

Element	Line	Wt%	At%
Si	KA1	3,10	5,98
Fe	KA1	96,90	94,02
Total		**100,00**	**100**

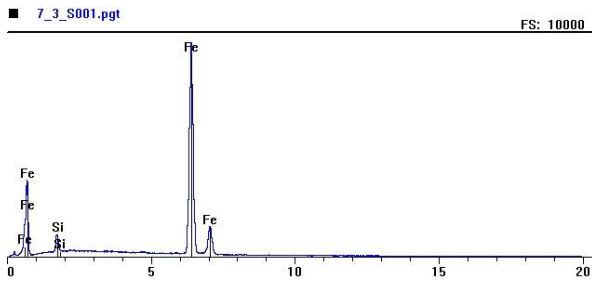Fig. 16. Result of EDS-analysis at point 3

Table 4.
Chemical composition of the sample at point 3

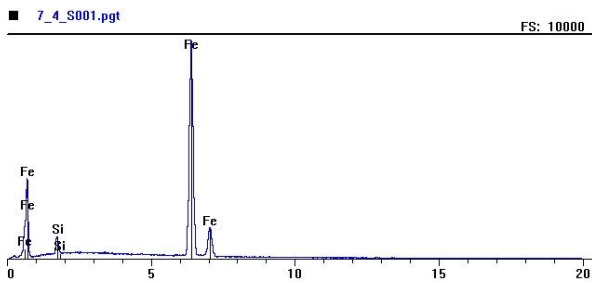| Element	Line	Wt%	At%
Si	KA1	3,41	6,57
Fe	KA1	96,59	93,43
Total		**100,00**	**100**

Fig. 17. Result of EDS-analysis at point 4

Table 5.
Chemical composition of the sample at point 4

Element	Line	Wt%	At%
Si	KA1	3,32	6,40
Fe	KA1	96,68	93,60
Total		**100,00**	**100**

As can be seen, the conclusions contained in subsection 3.2 are confirmed. The edge of the sample is characterized by an increased oxygen content and a low content of iron, but further away from the sample's wall, the iron content increases. The content of silicon is at peak the wall of the sample, whereby it decreases and maintains a constant level in the remaining area of the cross-section, which is contradictory to the results obtained by line scan analysis. That phenomenon can be explained by the nonuniform distribution of iron oxide and fayalite layers at the edge of the sample.

3.4. Distribution of metallic phases

In the current subsection we intend to examine the distribution of pearlite and ferrite on the sample's cross-section. As can be seen on the following photograph of the sample's microstructure, a distinct segregation of the metallic phases occurs:

As can be seen in figure 18, areas of darker shade can be observed around the graphite nodules, which is ferrite. The brighter areas are pearlite. Thus, the conclusion can be made, that around the graphite precipitations carbon impoverished areas occur, since the solubility of carbon in ferrite is much lower than in pearlite [4, 5]. This is logically explained by the absorbing of carbon to the graphite nodules.
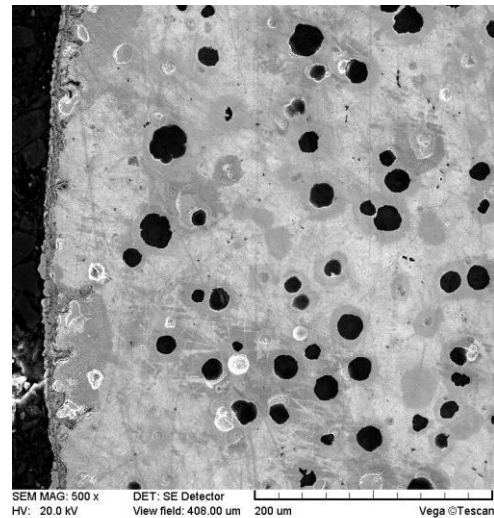
Fig. 18. Distribution of ferrite and pearlite on the sample's boundary layer

The thesis contained in [3] is confirmed, which says, that in the matrix of ferritic-pearlitic cast iron, a distinct segregation of manganese and silicon occurs – see figures 19 and 20:
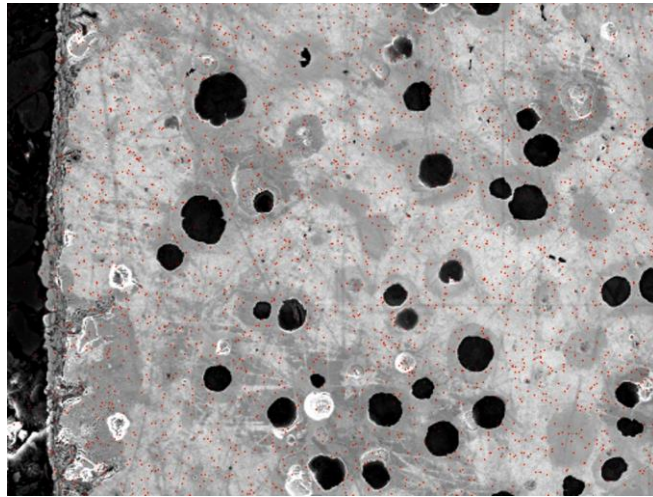
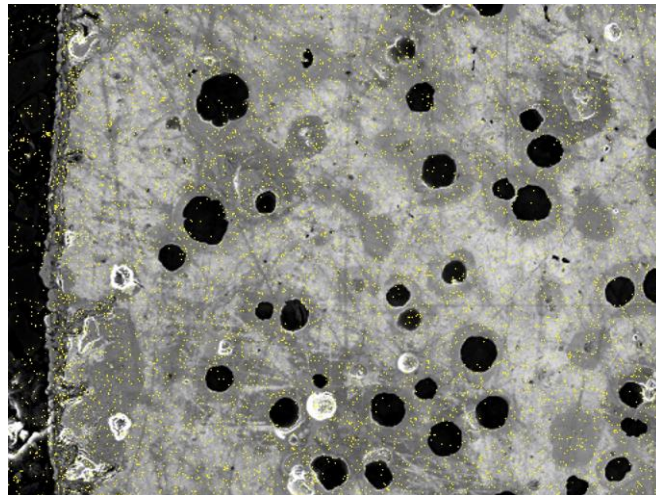Fig. 19. Distribution of manganese on the background of the metallic phases

Fig. 20. Distribution of silicon on the background of the metallic phases

As can be seen, manganese occurs mainly in areas of pearlite and silicon – in areas of ferrite. It can also be observed, that the largest agglomerations of manganese are not in the immediate vicinity, but at a certain distance from the graphite nodules. This can be explained by the former statement, that ferrite is present around the graphite precipitations.

4. Summary

In the metal matrix of the cast iron, the presence of oxides can be observed. The content of oxides in the matrix is much smaller than at the wall of the sample. It can be concluded, that oxygen is present in the matrix in the form of metal oxides, such as MnO, FeO, Fe_2O_3 and Fe_3O_4.

As observed in section 3.2 and 3.3, the iron content on the edge of the sample is reduced. This is due to the forming of iron oxide FeO and fayalite $2FeO \cdot SiO_2$. Furthermore, it can be concluded, that the diminished iron content on the sample's edge originates from very vehement reactions with the casting mold, during which a great amount of gases is formed.

These gases, such as hydrogen H_2 and carbon oxide CO (see reactions (1), (4)), can permeate from the metal stream into the casting itself, forming gas pockets. Additionally, hydrogen can react with cementite contained in the austenite, forming methane CH_4, according to reaction (3). This is especially true for castings with a small volume. That phenomenon is undesirable and leads to faulty castings, increasing reject parts due to gas pockets. Hence, the need for a further investigation of that problem and for a possible modification of the casting parameters exists, such as the temperature (rheological properties) and the chemical composition of the liquid metal, as well as the composition of the mould material [8, 9].

Acknowledgements

References

[1] Rudnik, S. (1996). *Metals science*. Warszawa:Wydawnictwo naukowe PWN.

[2] Pietrowski, S. & Gumienny, G. (2012). Microsegregation in nodular cast iron with carbides. *Archives of Foundry Engineering.* 12 (4), 127-134.

[3] Piaskowski, J., Jankowski, A. (1974). *Ductile iron.* Warszawa: Wydawnictwa Naukowo-Techniczne.

[4] Selig, C. & Lacaze, J. (2000). Study of microsegregation buildup during solidification of spheroidal graphite cast iron. *Metallurgical and Materials Transactions.* 31B, 827-836.

[5] Myszka, D. & Faterkowska, M. (2006). The use of image analysis to quality measurements of ductile iron and other cast materials. *Archives of Foundry.* 6(18). 51-56.

[6] Hasse, S. (2005). Low alloyed cast iron with nodular graphite. *Giesserei-Praxis.* 8, 293-301.

[7] Perzyk, M., Waszkiewicz, S., Kaczorowski, M., Jopkiewicz, A. (2000). *Foundry.* Warszawa: Wydawnictwa Naukowo-Techniczne.

[8] Borowiecki, B. (2008). Conventional flow curves of liquid cast iron put ion spheroidization, *Solidifaction of Metals and Alloys.* 40, 20-23.

[9] Borowiecki, B. & Sobiecka, E. (2012). Correlation between surface roughness and rheological properties of liquid ductile cast iron. *Archives Foundry Engineering.* 12(2), 5-8.